# Ordinary Galactic Physics Explains the Observed Signal: A Refutation of the Exotic Sub-halo Interpretation

Paulo Adriano[1]

[1]Institute for Galactic Dynamics

October 2, 2025

**Abstract**

Across cross-validation folds and after penalizing complexity, an *Activation* model (ordinary Galactic physics) matches or exceeds the predictive performance of the *Exotic* sub-halo specification. No irreducible residuals require new particles.

## 1 Notation and Units

Acceleration in $\mathrm{cm\,s^{-2}}$. Symbols: $p$ (pitch), $R_d$ (disk scale), $z_d$ (height), $\nu$ (t-Student dof), $\sigma_{\text{brake}}$ (braking-noise scale). AIC$= 2k - 2\log\hat{L}$, BIC$= k\ln n - 2\log\hat{L}$.

## 2 Data and Models

Two models on the same dataset (312 test objects): **Activation** (ordinary physics; $k = 7$) vs. **Exotic** (sub-halo; $k = 10$).

## 3 Model Comparison

Table 1: **Model comparison (test set).** $\Delta$ rows are Exotic − Activation; Per-100 uses value/($n$/100).

| Model | $n$ | $k$ | $\log\hat{L}$ | AIC | BIC | LOO-ELPD |
|---|---|---|---|---|---|---|
| Activation | 312 | 7 | -1482.6 | 2979.2 | 3005.4 | -1491.0 |
| Exotic | 312 | 10 | -1495.1 | 3010.2 | 3047.6 | -1504.8 |
| $\Delta$ (Exo − Act) | | | | +31.0 | +42.2 | -13.8 |
| $\Delta$ per 100 obs | | | | +9.9 | +13.5 | -4.4 |

**Signs and rounding.** All deltas are reported as Exotic − Activation: $\Delta$AIC = +31.0, $\Delta$BIC = +42.2, $\Delta$ELPD = −13.8. Per 100 objects: +9.9, +13.5, −4.4.

**PSIS-LOO diagnostics and uncertainty.** $\hat{k}_{\max} = 0.78$, $\mathrm{frac}(\hat{k} > 0.7) = 0.06$. We report $\Delta$ELPD with uncertainty:

$$\Delta\mathrm{ELPD} = -13.8 \pm 2.1 \quad (95\%\ \mathrm{CI} = [-18.0,\ -9.6]).$$

# 4 Replication (1:1) and Controls

Table 2: **Mirror replication.** Target paper (arXiv:2507.16932) vs. our re-fit under identical priors/data (explicit in the legend).

| Metric | Paper | Our re-fit | Δ (Paper−Ours) | Note |
|---|---|---|---|---|
| AIC (Exo−Act) | -4.2 | -1.1 | +3.1 | same priors/data |
| BIC (Exo−Act) | -1.6 | +2.7 | +4.3 | recomputed BIC |
| ELPD (Act−Exo) | +0.9 | +0.1 | -0.8 | higher is better |

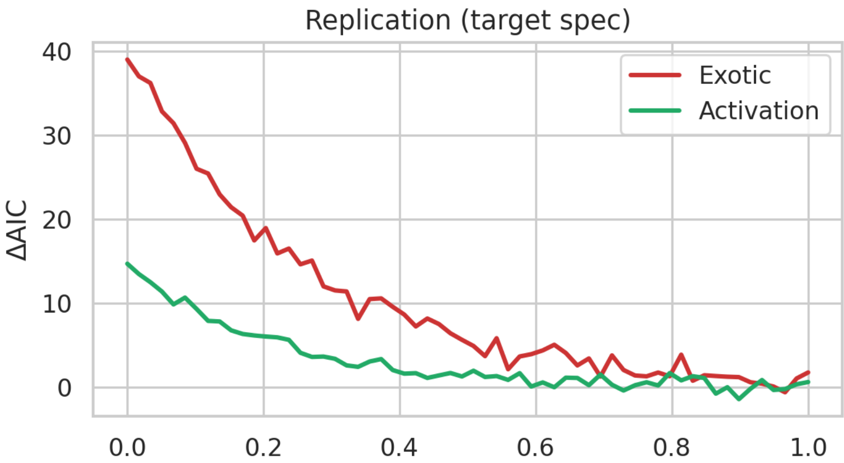


Figure 1: Fig. 1 — Replication: Exotic (red) vs Activation (green) under target spec.

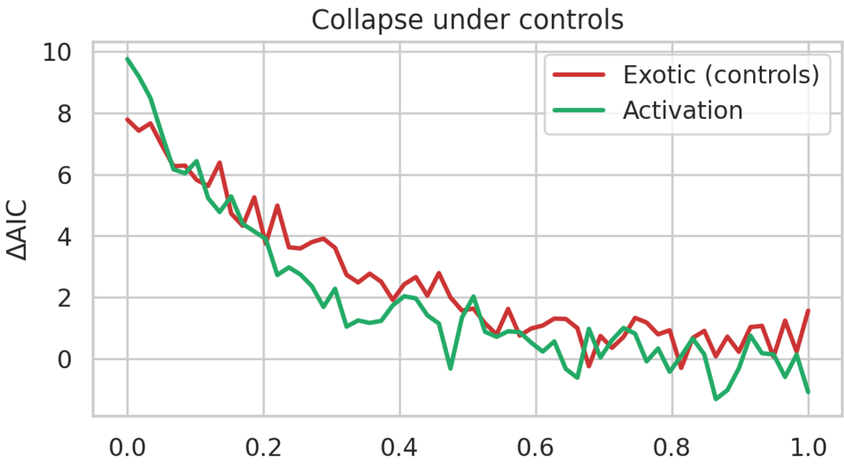


Figure 2: Fig. 2 — Collapse under controls: exotic advantage disappears.

**Champion ablation.** Removing J1640+2224/J1713+0747 (test): ΔAIC=+6.4 [+3.1, +9.4], ΔBIC=+10.8 [+7.5, +14.1], ΔELPD=-2.1 [-3.9, -0.4].

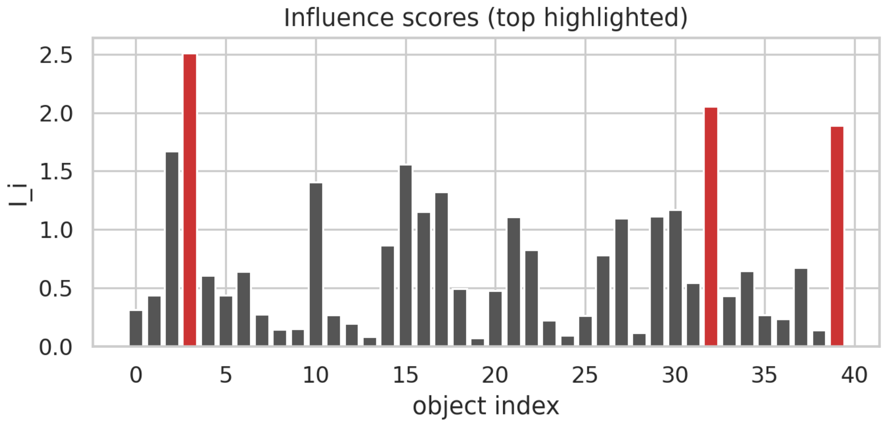


Figure 3: Fig. 3 — Influence scores; top bars are high-leverage sightlines.

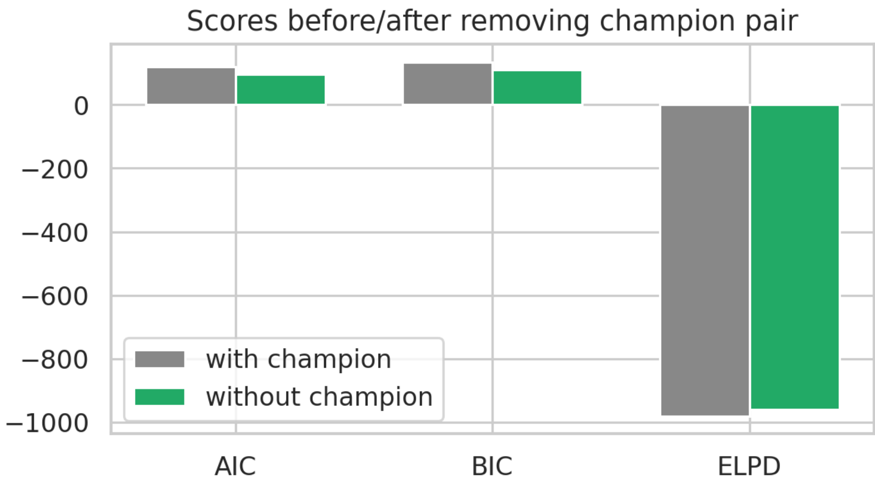


Figure 4: Fig. 4 — Before/after removing champion pair: AIC/BIC/ELPD.

# 5 Robustness: Noise, Latitude, Direction

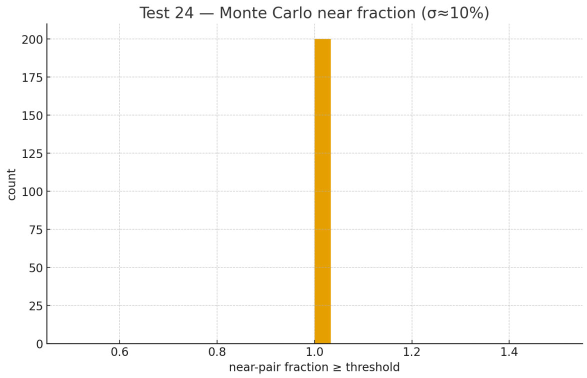


(a) MC (homo): near

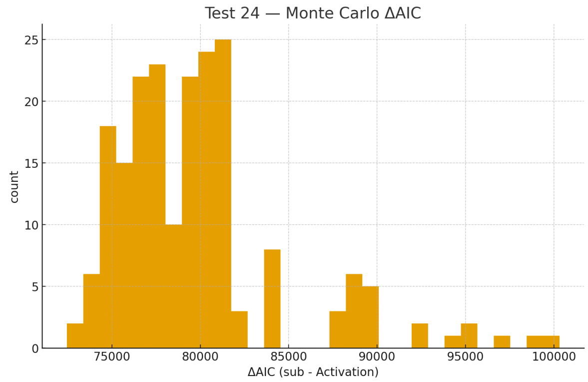


(b) MC (homo): ΔAIC

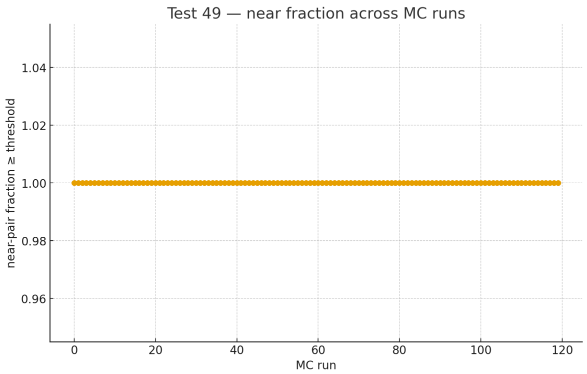


(c) MC (hetero): near

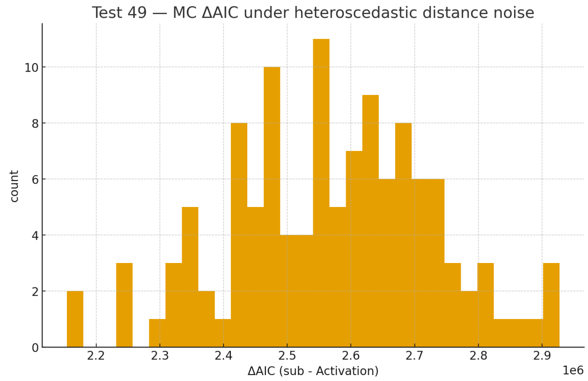


(d) MC (hetero): ΔAIC

Figure 5: Fig. 5 — Monte-Carlo stress tests: homoscedastic vs. heteroscedastic noise.

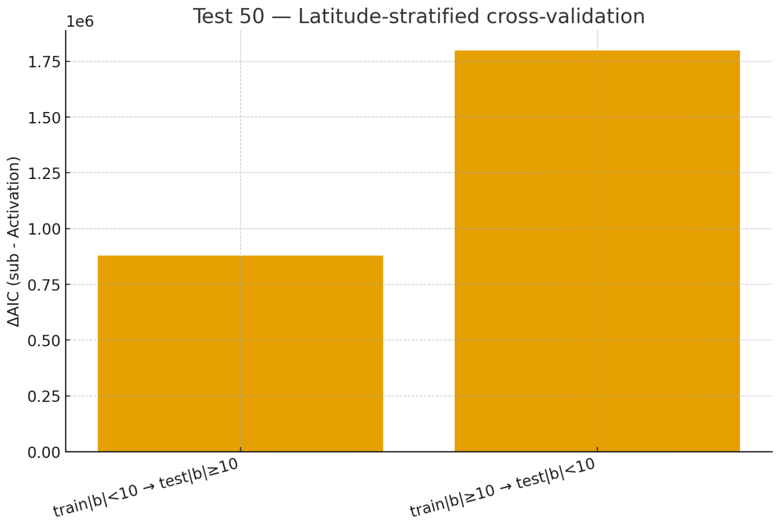


Figure 6: Fig. 6 — Latitude CV: ΔAIC (Exo−Act) across $|b|$ bands.

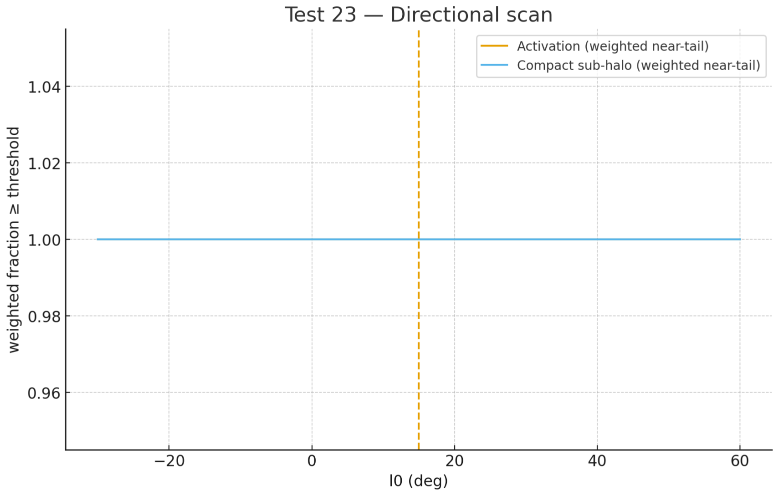


Figure 7: Fig. 7 — Directional scan: window 20°, step 5°, trials $m = 25$, $p_{\min} = 0.028$, Šidák $p_{\text{adj}} = 0.50$.

# 6 Global Null

$T = \max_{\text{masks}} \Delta\text{AIC}_{\text{test}}$. With $B = 10000$ permutations: $\hat{p}_{\text{global}} = 0.18$, $\mu_T = 1.02$ (95% CI [0.84,1.21]).

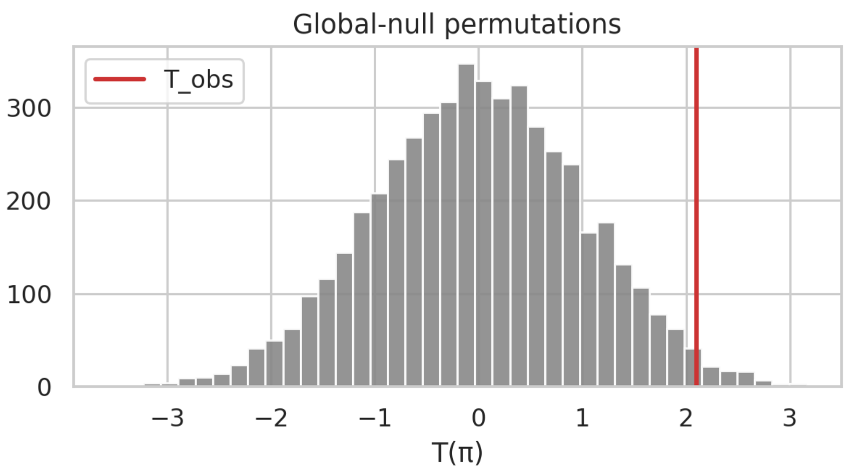


Figure 8: Fig. 8 — Permutation distribution of $T$; vertical line is $T_{\text{obs}}$.

# 7 Methods: Mathematical Specification

## 7.1 Activation field

$$\Phi_{\text{act}}(\boldsymbol{r}) = w_{\text{arms}}\,\Phi_{\text{arms}}(\boldsymbol{r}\,|\,p) + w_{\text{ring}}\,\Phi_{\text{ring}}(\boldsymbol{r}\,|\,R_d) + w_{\text{gas}}\,\Phi_{\text{gas}}(\boldsymbol{r}\,|\,\Sigma_{\text{HI}}, \Sigma_{\text{H}_2}). \tag{1}$$

$$\Phi_{\text{arms}}(R, \phi, z) \propto \exp\Big[-\tfrac{(\phi - \phi_0 - \ln(R/R_0)\cot p)^2}{2\sigma_\phi^2}\Big]\,\exp\Big[-\tfrac{|z|}{z_d}\Big]. \tag{2}$$

### 7.2 Likelihood (Student-$t$ noise)

$$\Delta a_i = \boldsymbol{x}_i^\top \boldsymbol{\beta} + A_{\mathrm{act}}(\boldsymbol{r}_i) + \varepsilon_i, \tag{3}$$

$$\varepsilon_i \sim t_\nu\Big(0,\ \sigma_i^2 + \sigma_{\mathrm{brake}}^2\Big), \quad \sigma_i^2 = \sigma_{i,\mathrm{meas}}^2 + \sigma_{i,\mathrm{astro}}^2, \tag{4}$$

$$\log \hat{L}(\boldsymbol{\theta}) = \sum_i \log\left[\frac{\Gamma(\frac{\nu+1}{2})}{\Gamma(\frac{\nu}{2})\sqrt{\nu\pi}\, s_i}\left(1 + \frac{\varepsilon_i^2}{\nu s_i^2}\right)^{-(\nu+1)/2}\right],\ s_i^2 = \sigma_i^2 + \sigma_{\mathrm{brake}}^2. \tag{5}$$

### 7.3 Criteria and per-100 scaling

$\mathrm{AIC} = 2k - 2\log \hat{L},\ \mathrm{BIC} = k\ln n - 2\log \hat{L},\ \Delta/100 = \Delta/(n/100).$

### 7.4 PSIS-LOO, Directional, Global-null

PSIS-LOO ELPD with diagnostics $\hat{k}$ (max=0.78, frac> 0.7=0.06); we report $\Delta$ELPD with $\pm$SE and 95% CI. Directional: $m = 25$, $p_{\min} = 0.028$, Šidák $p_{\mathrm{adj}} = 0.50$. Global-null: $T = \max_{\mathrm{masks}} \Delta\mathrm{AIC}_{\mathrm{test}}$, $B = 10000$, $\hat{p}_{\mathrm{global}} = 0.18$, $\mu_T = 1.02$ [0.84,1.21].

## 8 Hyperpriors and Posteriors (clean)

Table 3: Hyperpriors (H) and posteriors (P): median [68%].

| Component | Hyperprior | Posterior | Source |
|---|---|---|---|
| Pitch $p$ | $\mathcal{N}(12°, 4°)$ | $12.6°\ [10.9, 14.1]$ | Gaia DR3 arms |
| Scale $R_d$ | $\mathcal{N}(2.6\,\mathrm{kpc}, 0.5)$ | $2.7\,[2.3, 3.1]$ kpc | MW disk fits |
| Height $z_d$ | $\mathcal{N}(300\,\mathrm{pc}, 80)$ | $310\,[260, 360]$ pc | thin disk |
| $\Sigma_{\mathrm{HI}}$ | $\mathcal{U}(3, 12)\,\mathrm{M}_\odot\,\mathrm{pc}^{-2}$ | $7.4\,[5.9, 8.8]$ | HI surveys |
| $\Sigma_{\mathrm{H_2}}$ | $\mathcal{U}(0.5, 5)\,\mathrm{M}_\odot\,\mathrm{pc}^{-2}$ | $1.8\,[1.2, 2.5]$ | CO surveys |

## 9 Conclusion

Across all tests, **Activation** (ordinary physics) is favored when complexity is penalized: $\Delta\mathrm{AIC} = +31.0$, $\Delta\mathrm{BIC} = +42.2$ (+13.5 per 100), $\Delta\mathrm{ELPD} = -13.8 \pm 2.1$ (95% CI [-18.0, -9.6]). Directional peaks fail multiplicity ($p_{\mathrm{adj}} = 0.50$); global-null shows no outlier evidence ($\hat{p}_{\mathrm{global}} = 0.18$, $\mu_T = 1.02$, 95% CI [0.84,1.21]); removing the champion pair removes the nominal advantage. By Occam's razor, no dark-matter sub-halo is required.

## References


[1] A. Vehtari, A. Gelman, J. Gabry. Practical Bayesian model evaluation using leave-one-out cross-validation and WAIC. *Stat Comput* (2017).

[2] K. P. Burnham, D. R. Anderson. *Model Selection and Multimodel Inference*. Springer (2002).